

ト調査によると、最終結果が出るまでの間「何かの間違いであってほしい」、「母乳が出なくなった」、「最終結果が出るまで毎晩夫婦で泣いていた」、「出産を祝ってくれる人たちの中で孤独だった」、あるいは「珍しい病名を告げられて周囲に相談する人がいなくてとても不安だった」というような家族の気持ちが聞かれる。新生児 MS で異常を指摘された小児の正確な診断は不可欠であるが、同時に家族の心情に配慮したサポートが必要である。

(山口清次)

#### 文 献

- 1) 北川照房, 他: タンデムマス法による新生児マススクリーニングで見つかる有機酸・脂肪酸代謝異常症の理解のために, 特殊ミルク情報46号, 2010

## 新生児聴覚スクリーニング

### a. はじめに

現在難聴の子どもは1,000人に2~3人の割合で生まれると言われている。しかし難聴は目に見えない障害であり、周囲に気づかれず放置されると言葉は遅れ、人格形成に影響を及ぼすこともある。言葉はコミュニケーションのひとつの手段であり、これが障害されればコミュニケーションの選択肢の幅を狭めてしまうことにもなる。

新生児聴覚スクリーニングは、生まれたばかりの赤ちゃんを対象に言葉の発達やコミュニケーション能力の獲得に深く関わる先天性難聴などの障害を早期に発見し、適切な治療や療育に結びつけるための重要な検査として2000年に導入された。

### b. 新生児聴覚スクリーニングとその経緯

以前より、いかに早期に小児難聴を発見するかは重要なテーマの一つであった。しかし、新生児に対し客観的に簡便でしかも偽陽性、偽陰性をいかに低くするかは至難であった。

古くは1965年の Downs の聴性反射、1985年の Crib-O-Gram などがあるが偽陽性、偽陰性が高くスクリーニングとして新生児期の聴力検査には適さなかった。

1970年の ABR の発見は、客観的に聴力を評価できるという点からは画期的であったが、値段が高く時間がかかり、操作も複雑なためスクリーニングには不向きであった。しかし、1978年の OAE、1986年の自動 ABR の発見は、値段も安く、時間は数分、検査は容易に誰でも行うことが可能となり、全新生児に聴覚スクリーニングを可能とした。

このような中で、1998年に Yoshinaga, Itano が「新生児期に難聴が発見され生後6か

月までに補聴器をフィッティングして聴能学習をすると、その難聴の重症度や家庭の経済格差、人種差などにかかわらず言語発達が良好で、3歳になると正常児の90%近い高い言語能力を身につける」という論文を発表した。その結果、新生児聴覚スクリーニングはきわめて意義の高いものであることが世界的に認識されるようになり、日本では厚生労働省のモデル事業として、2000年度より自治体の手上げ方式で新生児聴覚スクリーニングが導入された。

## 6. 新生児期の聴覚検査（スクリーニング検査）

新生児期のスクリーニング検査は現在、産科、新生児科で施行するのが一般的であり、簡易で精度の高い検査として自動 ABR と OAE の 2 種類がある。いずれの検査も睡眠導入剤は必要なく、短時間に検査ができ操作もきわめて簡単で左右別々に難聴疑いか否かが客観的に評価できる。結果はシートで表示されるため容易に結果を理解できる。

なお、検査前には両親に難聴の発生頻度や、早期発見・早期教育の目的での聴覚スクリーニングについての説明を必ず行い、同意を得ることが必要である。

### 1) 自動 ABR：自動聴性脳幹反応（Automated Auditory Brainstem Response）

自動 ABR は音刺激をあたえ得られる聴性脳幹反応をアルゴリズムによって自動解析し結果が「Pass」、「要再検」とシートに表示されるものである。検査はカプラを耳に装着して行う。カプラから35dB（ささやき声程度の音圧）のクリック音を新生児に聴かせ、発生した ABR をあらかじめ検査機器に登録されている正常波形とのパターン・マッチングを行う。最大15,000回の刺激回数により判定が行われ、テンプレートと一致する波形が160回以上カウントされると「Pass」、160回未満であれば「要再検」と表示される。「Pass」の場合は正常とみなす。「要再検」の場合は40dB、70dB の 2 つの刺激音で再検査し、その結果も「要再検」であれば、退院前にもう一度自動 ABR で再検査する。

偽陽性は低く多くの場合1%以下である。偽陰性はゼロではないがきわめて低い。

### 2) OAE：耳音響放射（Otoacoustic Emissions）

OAE は DPOAE（Distortion Product OAE）と TEOAE（Transient Evoked OAE）がよく使用される。OAE とは耳音響反射と呼ばれ、外耳道にプローブを挿入して反応をみる検査方法である。これは、音響放射が鼓膜を通り内耳の蝸牛にある外有毛細胞の生体反応をとらえているものである。DPOAE は歪成分耳音響放射とよばれ、周波数別の評価が可能である。TEOAE は一過性誘発耳音響放射とよばれているもので、これは周波数別の判断はできない。

OAE は DPOAE、TEOAE とともに内耳の蝸牛にある外有毛細胞の生体反応をとらえているものあり、内耳（蝸牛）以降の難聴、すなわち後迷路性難聴の診断は不可能となる。したがって、Auditory neuropathy など内耳は正常であるが、聴神経の障害など内耳より中枢側に異常がある場合には OAE は正常な反応を示すため障害を検出できない。ちなみに自動 ABR は後迷路性難聴の診断も可能である。

また、OAE は自動 ABR と異なりプローブの挿入の仕方や耳垢などによって要再検率

が高くなるといった特徴があるため、最初の検査で「要再検」となった場合、2度3度と検査を繰り返し確認する。しかし値段が自動 ABR より安いことから使用されることが多く、OAE 検査にあたっては機器の特徴を熟知していることが望まれる。

#### d. 新生児聴覚スクリーニング検査の結果への対応

##### 1) スクリーニング検査で「Pass」例への対応

「Pass」の場合には、現時点では聴力に異常がないとして良いが、生後の成長過程でおこる、おたふくかぜや中耳炎による聴力障害や遅発性難聴は発見できないため、聴覚の発達に注意が必要であることを説明する。

##### 2) スクリーニング検査で「要再検」例への対応

「要再検」とは、もう一度検査の必要があることを示しているもので、直ちに聴覚障害があることを意味するものではない。説明は医師が、①聴覚検査での反応が不十分であったこと、②その詳細はその検査のみではわからないため、さらに詳しい検査を必要とすること、③精密検査は耳鼻咽喉科の医師のもとにすすめる、ということプライバシーに配慮したうえで説明することが望ましい。また、「今後どうなるのか」という不安も生じやすいため、精密検査実施機関を紹介する際は、具体的な受診方法や受診時期を説明するなど、今後の見通しを持った説明が必要である。

生後3か月以内に確定診断目的で、耳鼻咽喉科の学会認定専門医がおり、乳幼児の難聴の聴覚検査機器のある病院、あるいは診療所の耳鼻咽喉科に紹介する。日本耳鼻咽喉科学会が「精密聴力検査機関」として全国の施設を指定しているため、HPを参考にするとよい。

##### 3) 片側「要再検」例への対応

片側要再検の場合でも、健側耳の管理が重要となるため、耳鼻科医によるフォローアップが必要となる。中には耳鼻科的な治療の対象となる疾患もあり、症候群性の疾患や他の合併症を伴う疾患などは小児科医への紹介も必要になることがあるため、精密検査実施機関を紹介する。しかし、片側性は後に言葉の発達などの障害はまったく引き起こさないため、過度の不安を与えないことがきわめて重要である。

#### e. 新生児期の聴力検査（精密検査）

乳幼児の難聴の精密検査は耳鼻科的診察のほかに、① ABR、②行動反応聴力検査、③小児神経耳科学的発達検査などにより総合的に診断する。

ABRはヘッドホンを耳に装着して行われるものであり基本的には自動 ABRと同様であり誘発反応である。自動 ABRは反応波形をアルゴリズムで自動解析しているが、ABRは誘発反応によって得られた波形を約1,000回加算し平均処理している。ABRは、自動 ABRと異なり確定診断として、波形を細かく分析できることや、難聴の程度を知るうえでも必要不可欠であり新生児期の聴力検査として必須である。

行動反応聴力検査は目が覚めている状態で音に反応する身体反応を調べるもので、音の

大きさを変えて反応を調べ、もっとも小さな値を「閾値」として目安にする検査である。

これらの検査はいずれも長所と短所があるので、そのことを考慮に入れていくつもの厳密な検査を重ねて、総合的に判断する。また、成長とともに改善したり、悪化したりすることがあるので、注意深く経過観察をして確定診断をずる必要がある。

## f. 難聴児への療育と治療

聴力に問題があるとわかれば、補聴器装用は早くて4～5か月であることから、それまでは帝京大学名誉教授田中美郷による「母親に対するホームトレーニング（教育プログラム）」が基本となる。また、五感のバランスを有効活用するため、音楽、とくに骨振動を活用して少しでも音環境の存在に気づかせ、脳刺激をしていくために音楽療法を取り入れることもある。音楽療法には、早期発見（診断）された赤ちゃんとその家族に音楽を通じて楽しい雰囲気の中で、希望を持って子育てに臨める環境を提供できるひとつの手法でもある。

教育施設には、①難聴児通園施設、②地域の身障センター・療育センター、③ろう学校の3つの種類がある。しかし、療育施設間ではその方法や教育に偏り、バラツキがあり、混乱のもとになっている。どこも、最初は補聴器をつけて教育を始めるが、難聴がきわめて重く、補聴器の効果が乏しい子には、2歳前後を目安に人工内耳の手術をする。現在の人工内耳による効果は目を見張るものがあり、人工内耳をつけて適切な教育を受けた子は小学校に上がる頃にはほとんど健常児と変わりなく、よく聞いてよく話すことができるようになるが、知的障害のあるケースでは効果をあげることが難しいとされる。

## g. 新生児聴覚スクリーニングの普及

言語獲得や人格形成などの観点からも新生児聴覚スクリーニングは難聴児の早期発見はきわめて重要である。

しかし導入後約10年が経過した現在、新生児聴覚スクリーニング検査を受けた新生児の割合に比べ検査を施行している施設が少なく、精密検査項目は、ほとんどの施設でABRが主体であり、CTや先天性サイトメガロウイルス、ASSR、遺伝子検査を施行している施設はほとんどない。またそれぞれの精密検査機関で可能な検査には限界があり、検査機関の連携によりバラツキがないように調整する必要がある。精密検査機関から療育施設へ紹介する聴力レベルでもバラツキがみられるなど、その施行方法にも問題点が挙げられており、スクリーニングの普及とともに問題点の改善が急務となっている。

また就学時でのコミュニケーションの評価などのフォローも必要になってくることから、長期的に考えていかなければならない。

(坂田英明)

# 子育て支援 ハンドブック

チェック版

編集／日本小児科学会・日本小児保健協会・日本小児科医会  
日本小児科連絡協議会ワーキンググループ

Check

日本小児医事出版社



## 2. 健診のポイント

### 新生児聴覚スクリーニング

#### はじめに

難聴は目に見えない障害であり、周囲に気づかれず放置されると言葉は遅れ、人格形成に影響を及ぼすこともある。言葉はコミュニケーションのひとつの手段であり、これが障害されればコミュニケーションの選択肢の幅を狭めてしまうことにもなる。

新生児聴覚スクリーニングは、生まれたばかりの赤ちゃんを対象に、言葉の発達やコミュニケーション能力の獲得に深く関わる先天性難聴などの障害を早期に発見し、適切な治療や療育に結びつけるための重要な検査である。

わが国では1998年よりスクリーニング検査が始まった。早期発見が可能となったことで早期からの介入により言語発達などの面で大きな飛躍となった。一方、10年が経過し当初の問題とは別な問題点も明らかになってきた。具体的には就学後の評価である。難聴は早期に発見できても、その後の療育や教育などの遅いやかかわりかたにより必ずしも言語発達が伸びていない場合もあるからである。たとえば人工内耳についてである。せっかく人工内耳を行ってもあまり活用していないこともある。今後の新たな課題であり、難聴児の追跡調査などが必要であろう。

#### 新生児聴覚スクリーニングの歴史

- 1965 : Downs : 主観的検査法 (聴性反射)
- 1970 : ABR の発見
- 1978 : OAE の発見
- 1985 : Crib-O-Gram の導入
- 1986 : 自動 ABR 開発
- 1997 : 自動 ABR が日本に導入
- 1999 : 新生児聴覚スクリーニング実施

#### 新生児期の聴力検査

新生児に行う聴力検査として、簡易で精度の高い自動 ABR と OAE がある。

自動 ABR による結果シート

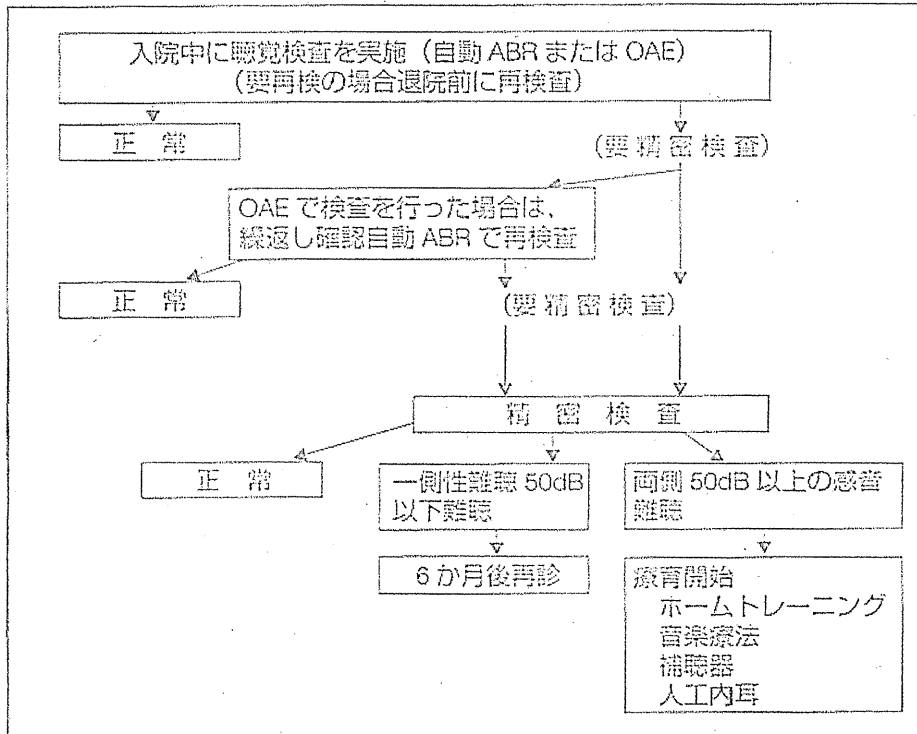
Netus-ALGO(R) 新生児用 ABR 聴力検査装置 検査結果	
姓名:	
医療記録番号:	
生年月日:	
性別:	男
日付:	14-Sep-2007
方法:	右/左 同勢
アプリケーション:	35dB nHL
検査時間:	09:54
聴覚混入率:	0%
右耳	パス
35 dB	挿引: 5000
左耳	要再検
35 dB	挿引: 15000

DPOAE による結果シート

ECHO<->SCREEN TDA *		ECHO<->SCREEN TDA *	
2006-08-14	OUT-Pat.	2009-12-01	OUT-Pat.
Examiner:		Examiner:	
DPOAE Result		DPOAE Result	
Left ear		Right ear	
10-10-14	11:20	10-10-18	10:53
A <sup>2</sup> S (L2=50dB SPL)		E77177 (L2=50dB SPL)	
2000Hz:	0 <sup>1</sup> 2	2000Hz:	E77177
2500Hz:	0 <sup>1</sup> 2	2500Hz:	E77177
3200Hz:	0 <sup>1</sup> 2	3200Hz:	E77177
4000Hz:	0 <sup>1</sup> 2	4000Hz:	E77177
コメント:		コメント:	

新生児聴覚検査の流れ

産科入院中に自動 ABR または OAE による聴覚検査を実施する。要再検の場合は退院前に再度検査を行う。この結果に異常が認められた場合は精密検査実施機関において精密検査を行う。聴覚障害と判断された場合は早期療育を開始する。尚 OAE の場合は後迷路性難聴（難聴全体の約 6%）の診断はできない為、パスとなっても難聴が存在する可能性がある。



新生児聴覚検査の流れ

リンパ節腫大の多くは非化膿性であるが、化膿性の場合には化膿レンサ球菌や黄色ブドウ球菌による感染であることが多く、またネコ引っかき病のこともある。反復性耳下腺炎では耳下腺部に腫瘤を生じる。

一方、無痛性で硬く可動性不良なリンパ節腫大、あるいは数か月にわたり改善しないリンパ節腫大では悪性腫瘍を疑う。悪性腫瘍としては悪性リンパ腫、神経芽腫、癌・肉腫のリンパ節転移がある。ただし、亜急性壊死性リンパ節炎でも腫脹は数か月に及ぶ。

図 診断

1. 問診, 身体所見 問診では腫瘤を自覚した時期, その後の大きさの変化, 自発痛・圧痛の有無に加え, 呼吸状態(気道圧迫による息苦しきの有無), 摂食状況について問い, 発熱の有無を確認する。腫瘤の部位, 性状〔硬さ, 波動の有無, 表面の状態, 可動性, 周囲組織との癒着の有無, 嚥下運動(喉頭挙上)との連動性〕をみる。扁桃炎などの上気道感染の有無, 耳下腺部の腫脹の有無についてもみる。息苦しさを訴える場合は, 必ず内視鏡で喉頭を観察する。

2. 検査 炎症性が疑われる場合は血液検査を行い, 適宜, 画像検査や病理検査を行う。先天性あるいは腫瘍性が疑われる場合は画像検査, 病理検査に加え, 適宜, 血液検査を行う。画像検査は超音波検査, CTを基本とし, MRIは必要に応じて撮る。病理検査として穿刺吸引細胞診を行う。

これら検査で確定診断に至らない場合は生検を行うが, その際は切開生検ではなく摘出生検を原則とする。血管腫では穿刺により血液が噴出することがあり, 血管腫が疑われる場合は穿刺を避ける。膿汁は検菌して起炎菌を同定する。

治療方針

図 先天性腫瘍

正中頸嚢胞, 側頸嚢胞では手術による全摘を行う。下咽頭梨状窩瘻は急性化膿性甲状腺炎を惹起するが, 抗菌薬の投与で消退しない

場合は切開排膿を要することもある。消炎を待って, 瘻管を甲状腺の一部とともに切除する。外切開を避けて, 内視鏡的に瘻管を焼灼して閉塞させることもある。嚢胞状リンパ管腫や血管腫ではエタノールやOK-432を注入する硬化療法を行う。

図 炎症性腫瘍

上気道炎や耳下腺炎などの原疾患の治療を行う。膿瘍を形成している場合は, 穿刺あるいは切開による排膿を行う。伝染性単核球症ではペニシリンは発疹を誘発するため禁忌である。

図 腫瘍

悪性リンパ腫では化学療法が主体となる。神経芽腫では手術, 化学療法を行う。甲状腺癌, 耳下腺癌, 上咽頭癌, 肉腫などでリンパ節転移を認める場合は, 手術, 放射線療法, 化学療法を原疾患に応じて単独あるいは組み合わせて行う。

好酸球性肉芽腫(木村病)ではステロイド, 抗アレルギー薬の内服を行う。

小児の補聴器装用とフィッティング  
amplification for infants and children  
坂田英明 目白大学保健医療学部教授・言語聴覚学科

言語習得前に生じた難聴は, 子どものきこえとことばの発達に影響し, さらに学力や社会生活にまで二次的に波及しうる。補聴器はきこえを補う最も実用的な手段の1つであり, 家族への説明と同意の上で, 言語習得に適した早期から装用を開始することが重要である。

近年, 新生児聴覚スクリーニング検査の普及によって難聴を早期に診断され, 0歳前半から補聴器の装用を開始する子どもの数が急速に増えている。人工内耳も含め, 補聴テクノロジーの技術進歩は著しく, 聴覚障害児が耳から音声言語を獲得する可能性は広がっている。



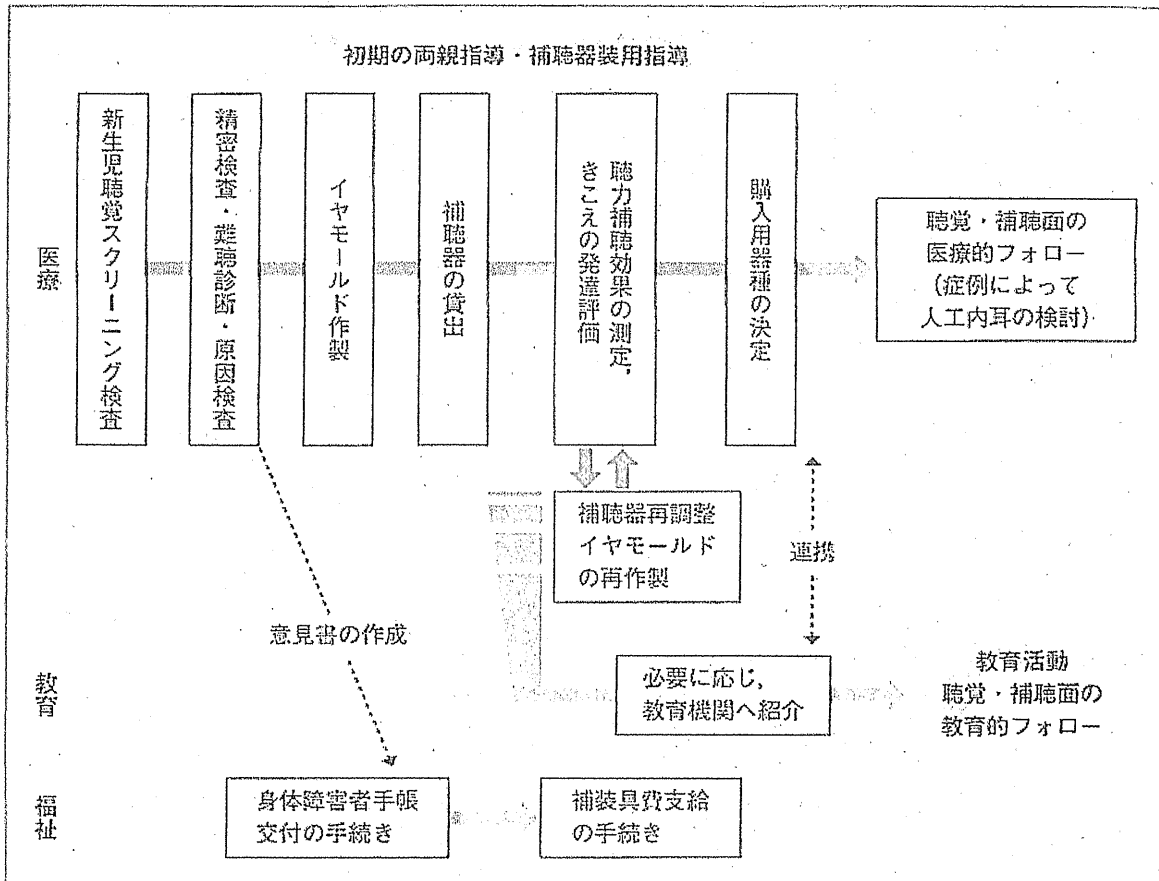


図1 子どもの補聴器フィッティングのプロセス

図 適応

会話音聴取に影響を与えるレベルの難聴が両耳にあれば、補聴器の適応と考えてよい。オーディオグラム上で40 dB以上の難聴があるか否かが一応の目安となる。多くは感音性難聴が適応となるが、伝音性難聴においても治療による聴力改善が困難な場合は適応となる。

図 補聴器のタイプと機能

補聴器の役割は音の増幅であり、音声を明瞭かつ快適に聴取できることが目標となる。子ども用としては、耳かけ形のタイプが一般的である。補聴器にはイヤモールドをつなぎ、外耳道に挿入する。耳介がまだ軟らかい乳児期においても、多くの場合、耳かけ形が適用可能である。耳あな形補聴器は、外耳が

成長期にある小児には推奨されない。耳介低形成や外耳道閉鎖を伴う伝音性難聴は、骨導補聴器の適用となる。

補聴器の基本的な調整機能として、利得/周波数特性、圧縮比、最大出力音圧レベルの設定がある。最近のデジタル補聴器は、雑音抑制、指向性、ハウリング抑制、音環境認識といった、さまざまな音環境下での聴取改善をめざした信号処理を行う器種も多い。価格は機能の高さにより、廉価のものから高価格のものまで幅広い。身体障害者手帳を交付されれば、購入費の一部が補助される。

図 フィッティング

乳幼児の補聴器特性処方は、推定聴力に基づいて行われる。聴力の推定は、他覚的検査と行動観察による幼児聴力検査から総合的に

行う。

他覚的検査法としては ABR(聴性脳幹反応聴力検査)が有用であるが, ASSR(聴性定常反応聴力検査)も参考にされる。

行動観察による幼児聴力検査法には, BOA(聴性行動反応聴力検査), COR(条件詮索反応聴力検査), VRA(視覚強化聴力検査), PA(遊戯聴力検査)があり, 発達状況に応じて検査法が選択される。

補聴器装用下の閾値測定や実耳測定も有用である。

#### 補聴器装用指導と教育

子どもの補聴器フィッティング(図 1)と装用指導は, きこえとことばの発達を促す教育活動のなかで行われることが望ましい。

初期の指導(主に両親指導)では, 補聴器の装用習慣と母子間の関わりの形成が重視される。

教育機関においては, 補聴援助システムの活用も必要である。聾学校や難聴幼児通園施

設などでは, 磁気ループや赤外線システムが使用される。一般学校の教室においては, FM 電波(169 MHz 帯)による補聴援助システムの利用が広まり始めている。

#### 補聴器特性処方例

新生児聴覚スクリーニング後の精査で, 推定聴力 90 dB の乳児。言語聴覚士により月齢 4 か月時に耳型採型を行い, 耳かけ形補聴器の両耳への貸出・試用を開始した。初期の特性は, 2cc カプラによる音響利得 40 dB(入力レベル = 60 dB SPL), フラットな周波数特性, 圧縮比 2:1, 最大出力音圧レベル 110 dB SPL に設定した。

両親指導と並行して, 聴性行動の発達的変化を観察しながら補聴器の再調整を続けた。8 か月時の VRA(インサートイヤホン使用)にて, 左右耳別の気導聴力を周波数別に測定できるようになり, 裸耳聴力/補聴効果がほぼ確定した。保護者・教育機関と相談の上, 購入用補聴器の器種を決定した。



ORIGINAL ARTICLE

# Topical application of the antiapoptotic TAT-FNK protein prevents aminoglycoside-induced ototoxicity

A Kashio<sup>1</sup>, T Sakamoto<sup>1</sup>, A Kakigi<sup>1</sup>, M Suzuki<sup>2</sup>, K Suzukawa<sup>1</sup>, K Kondo<sup>1</sup>, Y Sato<sup>3</sup>, S Asoh<sup>3</sup>, S Ohta<sup>3</sup> and T Yamasoba<sup>1</sup>

We previously demonstrated that an artificial protein, TAT-FNK, has antiapoptotic effects against cochlear hair cell (HC) damage caused by ototoxic agents when applied systemically. To examine the feasibility of topical protein therapy for inner ear disorders, we investigated whether gelatin sponge soaked with TAT-FNK and placed on the guinea pig round window membrane (RWM) could deliver the protein to the cochlea and attenuate aminoglycoside (AG)-induced cochlear damage *in vivo*. First, we found that the immunoreactivity of TAT-myc-FNK was distributed throughout the cochlea. The immunoreactivity was observed from 1–24 h after application. When TAT-FNK was applied 1 h before ototoxic insult (a combination of kanamycin sulfate and ethacrynic acid), auditory brainstem response threshold shifts and the extent of HC death were significantly attenuated. When cochlear organotypic cultures prepared from P5 rats were treated with kanamycin, TAT-FNK significantly reduced the extent of caspase-9 activation and HC death. These findings indicate that TAT-FNK topically applied on the RWM can enter the cochlea by diffusion and effectively prevent AG-induced apoptosis of cochlear HCs by suppressing the mitochondrial caspase-9 pathway.

Gene Therapy advance online publication, 22 December 2011; doi:10.1038/gt.2011.204

**Keywords:** protein therapy; apoptosis; cochlea; aminoglycoside; topical application

## INTRODUCTION

Apoptosis is involved in cochlear sensory hair cell (HC) death caused by a variety of insults, which include acoustic trauma, loss of trophic factor support, ischemia–reperfusion, and exposure to ototoxic agents such as aminoglycoside (AG) antibiotics and the anti-neoplastic agent cisplatin.<sup>1–3</sup> Protecting cells from apoptosis by controlling the balance of pro- and antiapoptotic proteins by techniques such as gene therapy is considered a good strategy for protection of HCs from ototoxic insults. Overexpression of Bcl-2 proteins by delivery of the *Bcl-2* gene into HCs has been reported to prevent the degeneration of HCs exposed to AG or cisplatin.<sup>4</sup> Injection of the *Bcl-x<sub>l</sub>* gene into mice cochlea also prevents HC degeneration induced by kanamycin.<sup>5</sup> However, such gene transfer application cannot control the amount or exposure time of the target protein to achieve optimal prevention of cell death. In addition, gene transfer technology cannot avoid the possibility of detrimental insertion of transgenes. Therefore, injection of the target protein could be an alternative method. For example, several proteins such as granulocyte-colony stimulating factor<sup>6</sup> have already been used in clinics. Such protein therapy, however, is not always applicable for treatment of inner ear disorders because the blood–labyrinth barrier may inhibit the delivery of high-molecular-weight proteins into the cochlea. This problem may be solved by using the protein transduction domain technology. When fused with a protein transduction domain such as the TAT domain of the HIV/Tat (transcription-transactivating) protein, a variety of high-molecular-weight proteins have been successfully introduced into cells both *in vitro* and *in vivo*.<sup>7,8</sup>

We first constructed a powerful artificial antiapoptotic protein, FNK (originally designated Bcl-xFNK by Asoh *et al.*<sup>9</sup>), which has

three amino-acid substitutions, Tyr-22 to Phe(F), Gln-26 to Asn(N) and Arg-165 to Lys(K), to strengthen the cytoprotective activity of Bcl-x<sub>l</sub>. We then demonstrated that fusion of FNK with TAT enabled FNK to penetrate highly negatively charged chondrocytes<sup>9,10</sup> and the blood–brain barrier,<sup>11</sup> and that TAT-FNK showed an antiapoptotic effect in a model of brain and hepatic ischemia.<sup>11,12</sup> When injected intraperitoneally into guinea pigs *in vivo*, we observed that TAT-FNK was distributed widely in the cochlea and that it reduced the expression of cleaved poly-(ADP-ribose)-polymerase (PARP), auditory brainstem response (ABR) threshold shifts, and HC loss induced by a combination of ethacrynic acid (EA) and kanamycin sulfate (KM), *in vivo*.<sup>13</sup>

Another potential drug delivery system for treatment of cochlear disorders is topical drug application into the middle ear space. Compared with systemic injections, such local delivery is beneficial because it requires significantly lower amounts of drug and reduces systemic side effects. A major side effect after long-term administration of an antiapoptotic drug is a possibility of carcinogenesis. Overexpression of Bcl-x<sub>l</sub>, the original protein of FNK, is reported to have the potential to cause tetraploidization, which would result in neoplasia.<sup>14,15</sup> Schuknecht<sup>16</sup> has developed a topical drug application technique for inner ear disorders: injection of streptomycin into the middle ear space of patients with Ménière's disease. Intra-tympanic dexamethasone injections have also been performed as primary treatment for sudden sensorineural hearing loss.<sup>17</sup> Intra-tympanic drug application has also been used in animal studies to examine the effects on inner ear function or disorders. It is quite difficult, however, to achieve the delivery of high-molecular-weight proteins into the inner ear because these proteins cannot pass through the round window membrane (RWM), which is the main route into the inner ear.

<sup>1</sup>Faculty of Medicine, Department of Otolaryngology and Head and Neck Surgery, The University of Tokyo, Tokyo, Japan; <sup>2</sup>Department of Otolaryngology and Head and Neck Surgery, Sakura Medical Center, Toho University, Chiba, Japan and <sup>3</sup>Department of Biochemistry and Cell Biology, Institute of Development and Aging Sciences, Graduate School of Medicine, Nippon Medical School, Kanagawa, Japan. Correspondence: Professor T Yamasoba, Department of Otolaryngology and Head and Neck Surgery, The University of Tokyo, Hongo 7-3-1, Bunkyo-ku, Tokyo 113-8655, Japan.  
E-mail: tyamasoba-tky@umin.ac.jp

Received 13 May 2011; revised 9 November 2011; accepted 14 November 2011

In the current study, we examined whether the TAT fusion technique could make transtympanic protein therapy applicable for inner ear disorders. We investigated whether TAT-FNK applied topically on the RWM could be successfully delivered into the cochlea, and protect cochlear HCs from an ototoxic combination of KM and EA. We also investigated whether TAT-FNK could prevent HC death caused by KM by suppression of the mitochondrial caspase-9 pathway.

## RESULTS

### Transduction of TAT-myc-FNK into cochlear tissue

Immunohistochemical staining using an anti-myc-tag antibody revealed that TAT-myc-FNK was detectable in the cochlea from 1 to 24 h after the application onto the RWM. There was a statistically significant difference between the groups as determined by one-way analysis of variance (ANOVA) ( $F_{6,203} = 41.239$ ,  $P < 0.01$ ). Scheffe's *post hoc* test revealed that the labeling indices (LIs) at 1, 3, 6, 12 and 24 h were significantly higher than that of the control ( $P < 0.01$ ). The LIs gradually increased from 1 to 6 h, but no differences were observed among the LIs at 1, 3 and 6 h. Beginning 12 h after the application, the LIs gradually decreased. The LIs at 6 and 12 h, 6 and 24 h, and 3 and 24 h were significantly different ( $P < 0.01$ ). No significant difference was observed between the LI of the control and that at 48 h (2a). High-power views of the organ of Corti (OC) and the spiral ganglion revealed that many spots consisting of TAT-myc-FNK were localized within the cells outside their nuclei (Figures 1b and c). The basal turn tended to show higher immunoreactivity than the upper turns, but there was no statistically significant difference between the cochlear turns at 1 and 6 h. Two-way ANOVA was conducted to examine the cochlear turns and the time course. There were no interactions between the two factors ( $F_{2,174} = 0.051$ ,  $P = 0.950$ ). There was also no statistical difference in the main effect of the cochlear turns ( $F_{2,174} = 1.033$ ,  $P = 0.358$ ; Figure 2b). In addition to the OC, the spiral ganglion cells (SGCs), the stria vascularis (SV) and spiral ligament (SL) also appeared to show greater

immunoreactivity than the control 6 h after the application of TAT-myc-FNK onto the RWM. Because the background immunoreactivity in the control sections varied between the organs, the normalized LIs, that is, the ratio of the LIs in each organ to those of the control, of these organs were compared by one-way ANOVA. There was a statistically significant difference between the groups ( $F_{3,116} = 39.257$ ,  $P < 0.01$ ). Scheffe's *post hoc* test revealed that immunoreactivity was strongest in the cells in the OC, followed by that in the SGCs. The normalized LI of the OC was significantly greater than that of the SGCs, the SV and the SL ( $P < 0.01$ ). The normalized LI of the SGCs was also significantly higher than that of the SV and the SL ( $P < 0.01$ ; Figure 2c). Specific immunoreactivity to myc was not observed in any control ears that were administered only myc-FNK (that is, without TAT) or in the ears of animals administered TAT-myc-FNK in the contralateral ear (Figure 1d).

### Protective effects of TAT-FNK against ABR threshold shifts induced by ototoxic insults

The baseline ABR thresholds measured before ototoxic insult were statistically not different at all tested frequencies among animals (data not shown). Neither experimental nor drug control animals showed any signs of systemic illness, such as diarrhea or hair loss, until euthanasia. For drug control animals, a gelatin sponge soaked with TAT-FNK was placed on the RWM, but a combination of KM and EA was not given. These animals showed no ABR threshold shifts at any tested frequency (data not shown), indicating that topical application of TAT-FNK on the RWM is not harmful to cochlear function.

ABR threshold shifts 14 days after the ototoxic insult in the experimental animals are shown in Figure 3 ( $n = 8$  each). Two-way ANOVA was conducted to examine the effect of the TAT-FNK administration and the frequency on the ABR threshold shifts. There was no significant interaction between TAT-FNK administration and hearing frequency ( $F_{2,42} = 0.042$ ,  $P = 0.959$ ). There was a main effect of TAT-FNK administration ( $F_{1,42} = 27.355$ ,  $P < 0.01$ ) but no significant difference in frequency ( $F_{2,42} = 0.833$ ,  $P = 0.442$ ).

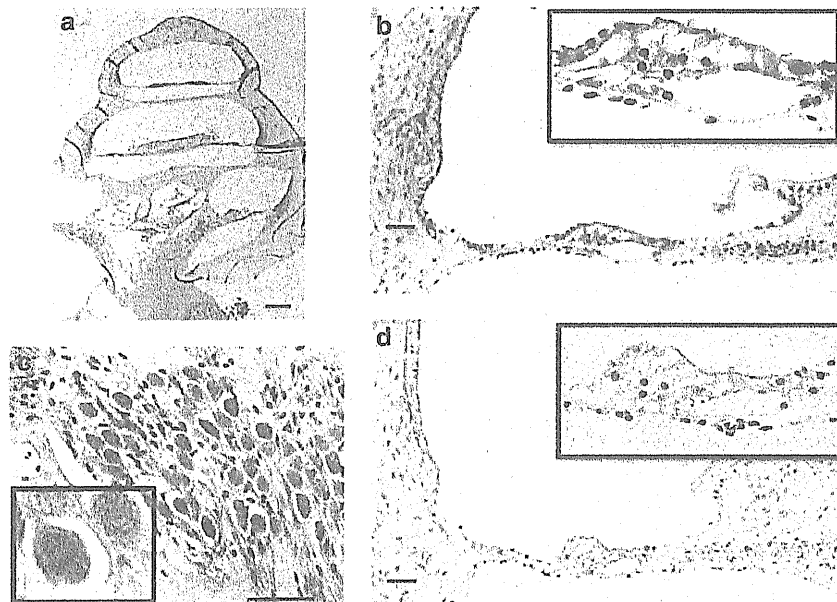


**Figure 1.** Transduction of TAT-myc-FNK protein into guinea pig cochlea. (a–c) The anti-myc-tag antibody was used to stain TAT-myc-FNK. Entire cochlea (a). An enlarged image of the OC (b) and the spiral ganglion (c). The insets in panels b and c are high-power views of the cells in the OC and SGCs, respectively. (d) An image of the contralateral ear, with a high-power view of OC in the insets. Scale bar: 200  $\mu$ m, panel a; 40  $\mu$ m, b–d.

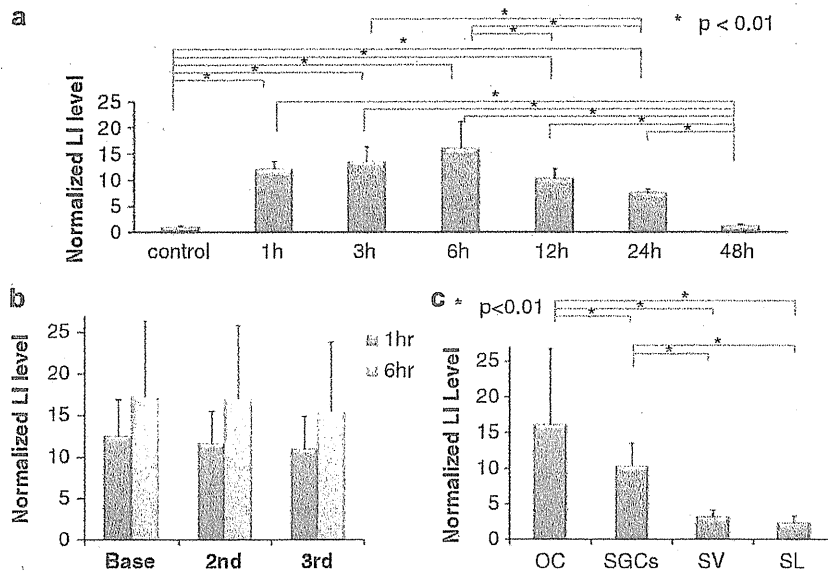


**Figure 2.** LIs for TAT-myc-FNK immunostaining of the inner ear. The time course of the normalized LIs level for immunostaining of the OC is shown (a). Error bar: s.d. \* $P < 0.01$ . (b) Normalized LIs for each turn at 1 and 6h after application of TAT-myc-FNK. (c) Normalized LIs at 6h for OC, SGCs, the SV and the SL. Error bar: mean (s.d.). \* $P < 0.01$ .

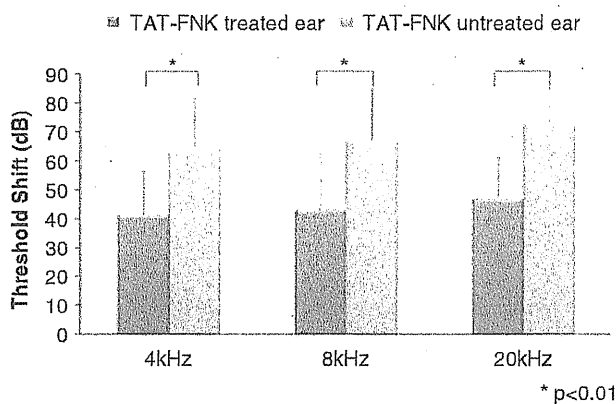


**Figure 3.** ABR threshold shifts at each tested frequency in both TAT-FNK treated and untreated ears. Pure tone 4, 8 and 20-kHz ABR threshold shifts before ototoxic insult and 14 days after the insult are shown. The dark gray bars indicate the values for the TAT-FNK-treated ears. The light gray bars indicate the values for the TAT-FNK-untreated ears. Error bar: s.d. \* $P < 0.01$ .

indicating that the ABR threshold shifts were significantly smaller at all the tested frequencies in the TAT-FNK-treated ears than in the untreated contralateral ears. This result suggests that the TAT-FNK treatment significantly attenuated the ABR threshold shifts induced by the ototoxic agents.

#### HC protective effects of TAT-FNK *in vivo*

Figures 4a and b show the average cytochrome c histograms in the TAT-FNK-treated and contralateral untreated ears, respectively, which were produced by plotting the average percentage of HC loss in every segment between 5 and 16 mm from the apex that was averaged across all subjects ( $n = 6$  each). Segments measuring under 5 mm and over 16 mm were excluded because the extent of HC damage could not be quantified owing to damage in some samples during surface preparation. The frequency map was added in the x-axis according to the data of Tsuji and Liberman.<sup>18</sup>

The ototoxic agents induced losses of  $91.7 \pm 7.0\%$  of the outer HCs (OHCs) and  $13.8 \pm 5.9\%$  of the inner HCs (IHCs) in the TAT-FNK-untreated ears, whereas the losses of the OHCs and the IHCs in the treated ears were reduced to  $64.0 \pm 29.6\%$  and  $8.3 \pm 3.5\%$ , respectively (Figure 4c). Two-way ANOVA was conducted to examine the effect of the TAT-FNK administration and the type of HC on HC loss. There was no significant interaction between TAT-FNK administration and type of HC ( $F_{1,20} = 3.055$ ,  $P = 0.096$ ). There were main effects of TAT-FNK administration ( $F_{1,20} = 6.869$ ,  $P = 0.016$ ) and type of HCs ( $F_{1,20} = 110.657$ ,  $P < 0.01$ ), indicating that the TAT-FNK treatment significantly attenuated the HC damage induced by KM and EA. Drug control animals administered only TAT-FNK showed minimal HC loss throughout the cochlea.

#### *In vitro* effect of TAT-FNK on protection of HCs and caspase-9 activation

Figure 5c shows an intact, untreated cochlear explant that was double-labeled with rhodamine-conjugated phalloidin (red) and activated caspase-9 (green). The stereocilia bundles on the three rows of OHCs and one row of IHCs have normal morphology and negligible green staining. Figure 5a shows a cochlear explant treated with KM for 10 h. HCs are missing and caspase-9 labeling is present in the HC regions. These results indicate that KM treatment caused an increase in caspase-9 activation, leading to apoptosis of the HCs by a mitochondria-mediated pathway. Addition of TAT-FNK to the explants greatly suppressed caspase-9 activation (Figure 5b). The number of HCs with activated caspase-9 in the explants treated only with KM was  $20.6 \pm 5.2$  per 0.2-mm length, whereas the number was reduced to  $7.6 \pm 3.2$  per 0.2-mm length in the explants treated with KM and TAT-FNK (Figure 5d,  $n = 4$  each). The number of HCs with activated caspase-9 in explants treated with KM and FNK (without TAT) was  $16.7 \pm 3.2$ . There was a statistically significant difference between the groups as determined by one-way ANOVA ( $F_{3,12} = 31.337$ ,  $P < 0.01$ ). Scheffe's *post hoc* test revealed that there were significant differences between the KM with TAT-FNK-treated explants, and the KM-treated explants or the KM with FNK-treated explants ( $P < 0.01$ ). There was no statistically significant difference between the KM-treated explants and the KM with FNK-treated explants

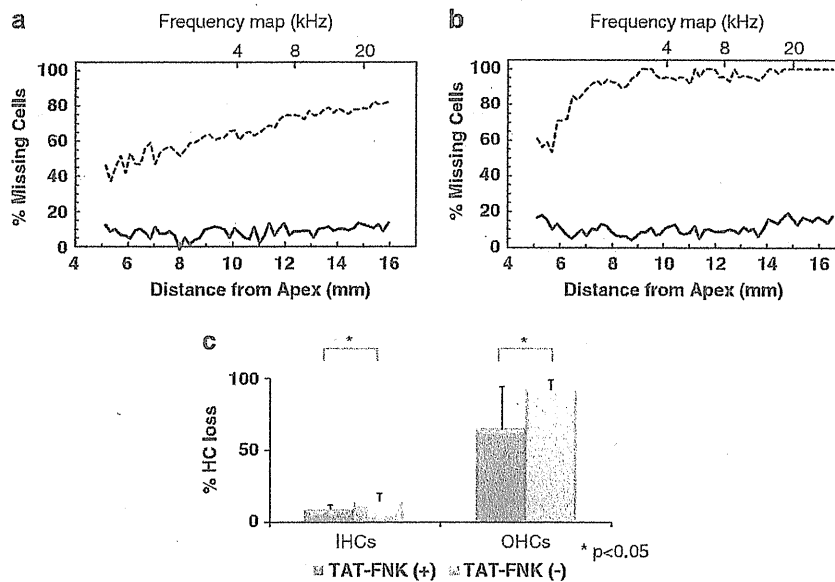


**Figure 4.** Average cytochleograms and average missing HCs for each experimental group 2 weeks after exposure to EA and KM. TAT-FNK-untreated ear (a). TAT-FNK-treated ear (b). The solid line represents the percentage of missing IHCs and the dashed line represents the percentages of missing OHCs. (c) The mean number of missing IHCs and OHCs from 5 to 16 mm. Error bar: s.d. \* $P < 0.05$ .

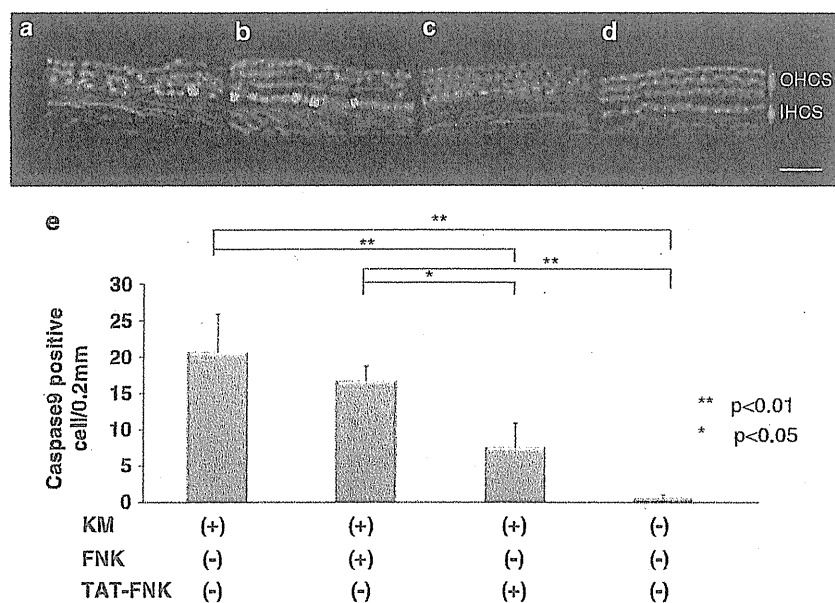


**Figure 5.** Fluorescence micrographs of caspase-9 activation and HC morphology. Rhodamine phalloidin (red) was used to stain the cell morphology and the fluorescent caspase substrate fam-LEHD-fmk (green) was used to stain caspase-9. Scale bar = 30  $\mu\text{m}$ . (a) TAT-FNK-untreated group. (b) FNK-treated group. (c) TAT-FNK-treated group. (d) Control group. (e) Mean number of caspase-9-positive HCs (IHCs + OHCs) present in 0.2-mm length of the cochlea. Error bar: s.d. \*\* $P < 0.01$ ; \* $P < 0.05$ .

( $P = 0.429$ ). Therefore, the TAT-FNK treatment significantly reduced the number of HCs entering the caspase-9-dependent apoptotic pathway after KM application.

We counted the number of viable HCs ( $n = 6$  each) after 12 h of culture. In the control that was not administered any additional agent such as KM, FNK or TAT-FNK, no or only few HCs were lost. When the number of viable HCs ( $n = 6$  each) was counted after 12 h of culture with KM (that is, in the absence of TAT-FNK), massive losses of the OHCs and the IHCs were induced, as only  $25.2 \pm 9.1\%$  and  $28.5 \pm 11.9\%$  of the cells survived, respectively. The TAT-FNK treatment attenuated OHC and IHC damages, as

$80.1 \pm 14.9\%$  and  $74.1 \pm 20.6\%$ , respectively, of the cells remained. In the explants treated with KM with FNK, the extent of survival was  $27.6 \pm 5.9\%$  for the OHCs and  $38.3 \pm 15.9\%$  for the IHCs. Two-way ANOVA was conducted to examine the effect of the drug administration and the type of HC on HC loss. There was a main effect of drug administration ( $F_{3,40} = 99.432$ ,  $P < 0.01$ ). There was also a main effect of type of HC ( $F_{1,40} = 419.899$ ,  $P < 0.01$ ). Finally, there was interaction between drug administration and type of HC ( $F_{3,40} = 47.846$ ,  $P < 0.01$ ). The simple effects analysis revealed significant differences between the KM with TAT-FNK-treated explants, and the KM-treated explants or the KM with FNK-treated

explants ( $P < 0.01$ ), in the OHCs. There was no significant difference between the KM-treated explants and the KM with FNK-treated explants. However, in the IHCs, there were no significant differences between the KM with TAT-FNK-treated explants, and the KM-treated explants or the KM with FNK-treated explants. These results indicate that the TAT-FNK treatment significantly attenuated damage to the OHCs; however, FNK alone did not protect the HCs against KM (Figures 6c and d). Drug control animals administered only TAT-FNK showed minor HC loss.

**DISCUSSION**

In the present study, we demonstrated that the TAT-fusion technique enabled the macromolecule FNK protein, which was infiltrated into a gelatin sponge and placed on the RWM, to successfully enter the cochlea because it allowed the protein to penetrate through the RWM. TAT-myc-FNK was distributed throughout all turns of the cochlea, but immunoreactivity was not observed in the contralateral ears, suggesting that, when topically applied, the distribution of TAT-FNK may be confined to the applied cochlea.

The Lis of TAT-myc-FNK gradually increased until 6 h, but there were no significant differences in the Lis at 1, 3 and 6 h. Beginning at 12 h, the Lis gradually decreased. At 48 h, the immunoreactivity disappeared. This suggests that TAT-myc-FNK was immediately distributed into the cochlea 1 h after administration onto the RWM and remained in high concentration until 6 h. It gradually decreased beginning at 12 h and disappeared by 48 h. When examining the entire cochlea at 6 h after administration of TAT-myc-FNK, the strongest immunoreactivity was present in the cytoplasm of the supporting cells and the HCs in the OC, followed by the SGCs. Immunoreactivity could also be observed in the SV and SL. This suggests that xTAT-myc-FNK was distributed most prominently in the OC followed by SGCs, and that it also

reached the SV and SL at 6 h after administration on the RWM. The duration of FNK expression was much longer compared with when it was administered systemically.<sup>13</sup> A single topical administration of TAT-FNK on the RWM effectively protected cochlear HCs from the combination of KM and EA *in vivo*. These findings imply that, when fused with TAT and soaked in a gelatin sponge macromolecular proteins can be applied on the RWM as an effective and selective therapeutic agent to function in the cochlea. Considering the adverse effects introduced by systemic injection, this technology is feasible as a novel treatment for inner ear disorders. TAT-FNK attenuated KM-induced HC death by suppressing the activation of pro-caspase-9 *in vitro*, suggesting that the antiapoptotic protein FNK has the potential to regulate the mitochondria-related apoptotic pathway in the inner ear.

The RWM is a main gate and barrier for various kinds of substances to enter from the middle ear into the inner ear.<sup>19</sup> The membrane consists of three layers: an outer epithelium facing the middle ear, a core of connective tissue and an inner epithelium facing the inner ear.<sup>20-22,16-18</sup> The structure of the outer epithelium is such that substances can pass from the middle to the inner ear by selective absorption and secretion.<sup>23</sup> The factors influencing permeability through the RWM include the molecular weight and configuration of the protein, its contact time and the concentration of the substances in the middle ear.<sup>23-25</sup> Among these, molecular weight is the most important in determining permeability. Generally, low-molecular-weight compounds, such as antibiotics, corticosteroids and labeled ions, can easily pass through the RWM to enter the inner ear,<sup>26,27</sup> whereas penetration of high-molecular-weight substances, such as proteins and lipids, is limited.<sup>19,27-30</sup> In the current study, myc-FNK, whose molecular weight is about 30 kDa, did not pass through the RWM, suggesting that it is too large to pass through. Many proteins related to apoptosis, such as p53, AKT and super oxide dismutase, have a molecular weight of 30-60 kDa. Thus, when considering the

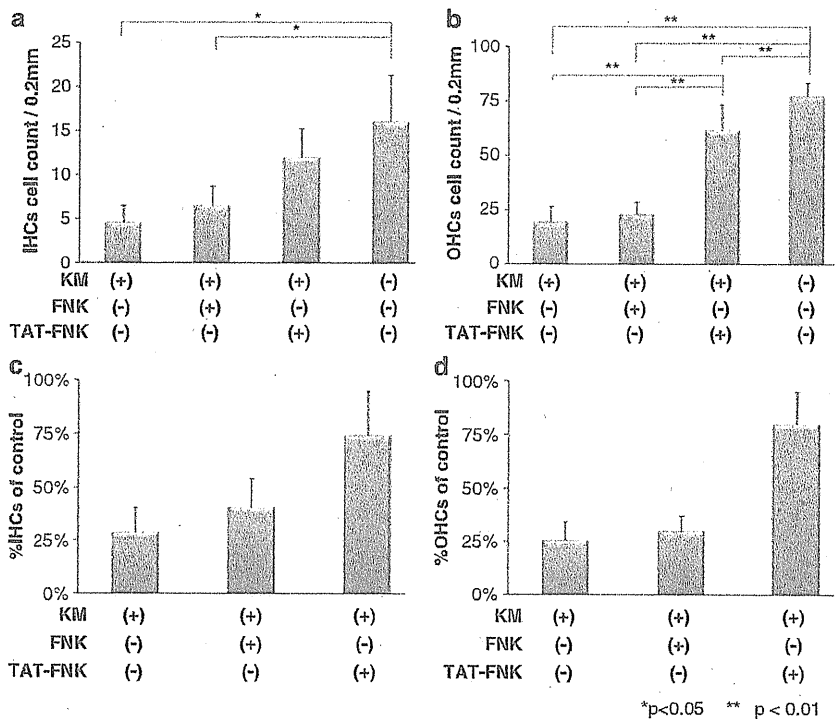


**Figure 6.** Mean number of surviving HCs of cultured OC after exposure to KM. The mean number of IHCs (a) and OHCs (b) present in a 0.2-mm length of cochlea taken from four independent parts of the middle cochlear section. Mean percentage of IHCs (c) and OHCs (d) relative to control cultures. Error bar: s.d. **\*\*** $P < 0.01$ ; **\*** $P < 0.05$ .



applicability of protein therapy from the middle ear space, new technology is required to overcome the difficulty of delivering large molecules to the inner ear. The Tat protein of HIV-1 is a protein of 101 residues. The Tat protein has the characteristic that it can cross the plasma membrane of neighboring cells.<sup>31</sup> TAT comprises the short stretches of the Tat protein domain that are primarily responsible for their translocation ability, also referred to as protein transduction domains.<sup>32</sup> Although the exact mechanism has not been elucidated, two models have been proposed: energy-dependent macropinocytosis, and direct uptake by electrostatic interactions and hydrogen bonding.<sup>33</sup> By fusing FNK to the TAT domain, FNK was effectively absorbed into the outer epithelium cells and then secreted to the inner ear space, although further studies are needed to confirm this. When fused with TAT, various proteins were reported to be transported across cell membranes.<sup>7,8</sup> Even  $\beta$ -galactosidase, whose molecular weight is 120 kDa, has been reported to enter cells.<sup>33</sup> Moreover, oligonucleotide, nucleic acids and liposome can also be conjugated with TAT to improve its penetration.<sup>34</sup> Thus, protein transduction technology allows the use of macromolecules for therapeutic application in a variety of inner ear disorders.

In our previous study, we successfully delivered TAT-FNK protein to the inner ear by intraperitoneal injection.<sup>13</sup> However, systemic administration may not be suitable for treatment of inner ear disorders because only relatively small amounts of drug can enter the inner ear, which therefore requires the application of high doses of drug to maintain a therapeutic concentration in the inner ear at an optimal time. Moreover, a single administration has a short half-life, as shown in our previous study,<sup>13</sup> and thus repeated administration is required. High doses of drug may easily induce systemic toxicities and acute allergic side effects. In particular, high doses of this antiapoptotic protein may promote tumor, although this has not been reported. Therefore, injection of drugs topically into the middle ear space may be more appropriate to better control local drug delivery. Injection of drugs into the middle ear space, however, may result in a large portion of the drug being absorbed by the middle ear mucosa or drained into the epipharynx by the Eustachian tube.<sup>35</sup>

To deliver a drug more effectively into the inner ear, using an absorbable material as a drug carrier may be promising. These materials could secure the stability of drugs on the RWM, and thereby lengthen the contact time with the RWM, and reduce diffusion into the mucosa and drainage from the middle ear space.<sup>36</sup> In the current study, we used a gelatin sponge as a carrier of TAT-FNK, as Husmann *et al.*<sup>37</sup> used a gelatin sponge on the RWM to topically apply gentamicin, which then induced severe damage to the cochlea compared with a single application. Similarly, Okamoto *et al.*<sup>38</sup> used a gelatin sponge containing bone morphogenetic protein-2, and demonstrated that bone morphogenetic protein-2 was slowly released and induced successful regeneration of cartilage in a canine tracheomalacia model. Compared with our previous systemic study,<sup>13</sup> we could observe immunoreactivity of TAT-myc-FNK in the cochlea using approximately 1/600th the amount of TAT-myc-FNK. Immunoreactivity of TAT-myc-FNK could still be observed in the cochlea after 24 h, which is significantly longer than the expression periods observed in previous systemic injection studies targeting organs, including the cochlea.<sup>11,13</sup> Further, the amount of TAT-FNK we topically applied to protect HCs from ototoxicity was approximately 1/15th the dose we used systemically to protect from the same ototoxicity in our previous study.<sup>13</sup> Thus, a gelatin sponge is considered to be an effective drug carrier for inner ear disorders.

When drugs are topically applied onto the RWM, they diffuse from the basal end of the cochlea and thus initially show a concentration gradient, decreasing toward the apex. The concentration gradient in the perilymph was investigated, and the greater concentration was demonstrated at the basal turn.<sup>39,40</sup> However, when the patterns of distribution of the drugs applied

on the RWM were investigated by immunocytochemistry, the drugs appeared to be widely and rapidly distributed into the various organs of the inner ear. Imamura and Adams<sup>40</sup> examined the distribution of gentamicin in the inner ear of guinea pig using a monoclonal antibody. When gentamicin was placed on the RWM, the entire cochlear cell was diffusely stained until 6 h after administration. Beginning at 6 h after application, staining was found to be localized mainly in the basal turn. Greater staining in the basal turn was also found when gentamicin was administered systemically. These results suggest that gentamicin can be diffused rapidly into the entire cochlea, and that the localization of staining in the basal turn is due to the nature of the cells in the basal turn to accumulate the drug, and not because of the predominant distribution of gentamicin at the basal turn. Zou *et al.*<sup>42</sup> examined the distribution of lipid nanocapsules in cochlear cells after application on the RWM by using fluorescein isothiocyanate and rhodamine-B labeling. The lipid nanocapsules were present in the SGCs, OC and SV 30 min after application. Moreover, the nanocapsules were more strongly distributed in the SV in the second turn than in the basal turn. They assumed that after penetrating the RWM, the nanocapsules are rapidly diffused through the porous modiolar wall of the scala tympani, after which they enter the SGCs, and then are widely diffused through its nerve fibers. In the present study, although there was a trend of higher intensity of immunoreactivity of TAT-myc-FNK at the basal turn, we did not observe statistically significant differences among the turns. We assume that this rapid and relatively even distribution of TAT-FNK throughout the cochlea was achieved by this radial diffusion through the modiolus, and not by longitudinal perilymph diffusion. Pathways to uptake lipid nanocapsules and TAT-mediated particles into the tissue might be similar, as their high permeability is considered to accelerate their rapid diffusion.<sup>41,42</sup> High immunoreactivity in the SGCs compared with those in the SV and SL at 6 h can support this argument, although the cause of the higher immunoreactivity in the OC compared with that in the SGCs needs to be clarified in future research.

It is known that high-frequency hearing loss occurs initially after AG ototoxicity. However, when the damage by AG is severe, apical cells will be affected and hearing loss expands to lower frequencies.<sup>43</sup> The doses of the KM and EA combination we chose were assumed to be sufficient to cause threshold shifts even at a low frequency. We observed some tendency that the OHCs in the basal parts are more susceptible to the combination of EA and KM than those the upper parts (Figures 4a and b). This finding is consistent with that in other studies.<sup>44</sup> When we compared the extent of missing HCs in the region corresponding to the frequency at which ABR was measured, the percentages of missing OHCs was approximately 67% in the region corresponding approximately to 4 kHz and 80% in that corresponding to 20 kHz. In untreated ears, the percentages of missing OHCs in the regions comparable to 4 and 20 kHz were 95% and 100%, respectively. The differences in the extent of OHC loss between the 4- and 20-kHz regions were small, supporting the ABR findings that there was no significant difference in the threshold shifts among the tested frequencies, although the ABR threshold shifts were slightly greater at higher frequencies than at lower frequencies.

In the current study, we showed that caspase-9 was activated by KM *in vitro*. This finding suggests that KM-induced cochlear HC death is caspase-9-dependent, which is consistent with other studies.<sup>1,45</sup> We demonstrated that TAT-FNK suppressed the activation of caspase-9 in this study and reduced the extent of cleaved PARP in OHCs in our previous study,<sup>13</sup> which suggests that TAT-FNK prevents the intrinsic apoptotic pathway, as does the parent protein Bcl-x<sub>L</sub>. It has also been shown that TAT-FNK affects the cytosolic movement of Ca<sup>2+</sup> and protects neuronal cells from glutamate excitotoxicity.<sup>11</sup> It has been shown *in vitro* that AG antibiotics cause an increase in intracellular calcium levels



in avian HCs<sup>46</sup> and in isolated OHCs of guinea pigs.<sup>47</sup> Therefore, inhibition of  $\text{Ca}^{2+}$  homeostasis distribution may have a crucial role in the ability of TAT-FNK to prevent apoptotic cochlear HC death. The mechanism of how TAT-FNK prevents cochlear HC death remains to be fully elucidated.

In conclusion, we demonstrated that TAT-FNK infiltrated in gelatin sponge and placed on the guinea pig RWM could successfully deliver the protein to the cochlea by penetrating through the RWM, and that a single topical administration of TAT-FNK protected the cochlea against the combination of the ototoxic drugs KM and EA *in vivo*. An *in vitro* study demonstrated that TAT-FNK suppressed the activation of caspase-9 and protected cochlear HCs from KM-induced apoptosis. These findings suggest that topical administration of an antiapoptotic protein fused with TAT and soaked with a gelatin sponge is effective at preventing the apoptosis of cochlear HCs, and that such topical treatment is superior to systemic administration in terms of organ specificity and safety. Future studies using this technology may extend the feasibility of protein therapy for treatment of inner ear disorders.

## MATERIALS AND METHODS

The experimental protocol was approved by the University Committee for the Use and Care of Animals at the University of Tokyo, and it conforms to the NIH Guidelines for the Care and Use of Laboratory Animals.

### Construction and preparation of TAT-FNK and TAT-myc-FNK

We constructed FNK (originally designated as Bcl-xFNK) by introducing amino-acid substitutions into Bcl-xL using a two-step PCR mutagenesis method, as reported previously.<sup>9</sup> The substituted codons were as follows: Tyr-22 (TAC) with Phe (TTC), Gln-26 (CAG) with Asn (AAC) and Arg-165 (CGG) with Lys (AAG). Among the mammalian antiapoptotic factors, FNK is the only mutant with a gain-of-function phenotype because, compared with Bcl-xL, FNK showed stronger antiapoptotic activity to protect cultured cells from death induced by various death stimuli, including oxidative stress, a calcium ionophore and withdrawal of growth factors.<sup>9</sup> TAT-FNK and TAT-myc-FNK were then prepared as described previously.<sup>11</sup> The gene constructed for FNK was fused with an oligonucleotide encoding TAT, and the resulting TAT-FNK gene encoded met-gly-TAT (consisting of 11 amino acids: YGRKKRRQRRR-gly-FNK. An oligonucleotide encoding GEQKLI-SEEDLG (the myc TAG sequence is underlined) was inserted between the TAT and FNK sequences of TAT-FNK by PCR to obtain TAT-myc-FNK. To construct myc-FNK without the TAT domain, an oligonucleotide encoding met-gly-myc TAG-gly was also ligated to the FNK sequence by PCR. The TAT-FNK plasmid was introduced into *Escherichia coli* DH5a cells (Invitrogen, Life Technology, Carlsbad, CA, USA) and the TAT-FNK protein was overexpressed by treatment with 1 mM isopropyl 1-thio- $\beta$ -D-galactoside for 5 h with vigorous shaking at 37 °C. Proteins were solubilized in buffer (7 M urea, 2% sodium dodecyl sulfate, 1 mM dithiothreitol, 62.5 mM Tris-HCl (pH 6.8) and 150 mM NaCl) and then subjected to sodium dodecyl sulfate-PAGE to remove contaminating proteins and endotoxins. The gel was treated with 1 M KCl and the transparent band corresponding to TAT-FNK was cut out. Proteins were electrophoretically extracted from the gel slice using extraction buffer (25 mM Tris, 0.2 M glycine and 0.1% sodium dodecyl sulfate) for *in vitro* and *in vivo* experiments. The extraction buffer was used as the vehicle. The concentration of the extracted TAT-FNK ranged from 1 to 6 mg ml<sup>-1</sup>.

### Immunohistochemical detection of TAT-myc-FNK in the cochlea after tympanic administration

Eighteen male albino guinea pigs (Saitama Experimental Animals Supply Co. Ltd, Saitama, Japan) weighing 250–300 g were used. Under anesthesia with xylazine hydrochloride (10 mg kg<sup>-1</sup>; Bayer, Leverkusen, Germany) and ketamine hydrochloride (40 mg kg<sup>-1</sup>; Sankyo, Tokyo, Japan), a post-auricular incision was made and the bone posterior to the tympanic ring was exposed. A hole was drilled into the bulla exposing the middle ear

space medial to the tympanic ring. The round window niche and the RWM were identified. The gelatin sponge (Sponge; Astellas Pharma Inc., Tokyo, Japan) was soaked in 3  $\mu$ l of TAT-myc-FNK (0.5 mg ml<sup>-1</sup>) and placed on the RWM of the left ear. The animals were killed at 1, 3, 6, 12, 24 and 48 h ( $n=3$  for each time point) after injection, while under deep anesthesia, using an overdose of xylazine hydrochloride (Bayer) and ketamine hydrochloride (Sankyo). Three animals that were killed 6 h after a similar tympanic administration of myc-FNK (3  $\mu$ l; 0.5 mg ml<sup>-1</sup>) served as controls. The cochleae from both ears were perfused with 4% paraformaldehyde in 0.1 M phosphate-buffered saline (PBS) at pH 7.4 through the oval and round windows, and immersed in the same fixative overnight at 4 °C. The specimens were decalcified in 10% EDTA acid for 14 days, dehydrated through a graded alcohol series and embedded in paraffin. The embedded tissues were cut into 5- $\mu$ m-thick sections parallel to the modiolus and mounted on glass slides. The sections were deparaffinized, hydrated and rinsed with PBS. To detect TAT-myc-FNK and myc-FNK *in situ*, rabbit anti-myc-tag polyclonal antibody was used (1:5000, 4 °C overnight; Upstate Biotechnology, Lake Placid, NY, USA) coupled with a DAKO Envision+ system (Dako Japan, Kyoto, Japan). Negative controls were established by replacing the primary antibody with blocking buffer.

The LI of the anti-myc antibody in the cochlear tissues was obtained by a modified Photoshop-based image analysis. The original method was developed by Lehr *et al.*<sup>48</sup> In brief, an image was digitized on magnetic optical disks. Using the 'Magic Wand' tool in the 'Select' menu of Photoshop, the cursor was placed on a portion of the immunostained area. The tolerance level of the Magic Wand tool was adjusted so that the entire immunostained area was selected. Using the 'Similar' command in the 'Select' menu, all the immunostained areas were selected automatically. Subsequently, the image was transformed to an 8-bit grayscale format. An optical density plot of the selected areas was generated using the 'Histogram' tool in the 'Image' menu. The mean staining intensity and the number of pixels in the selected areas were quantified. Next, the background was selected using the 'Inverse' tool in the 'Select' menu. The mean background intensity was quantified using the 'Histogram' tool as mentioned above. The immunostaining intensity was calculated as the difference between the mean staining intensity and the mean background intensity. The immunostained ratio was calculated as the ratio of the number of pixels in all the immunostained areas to that in the entire image. LI was defined as the product of the immunostained ratio and the immunostaining intensity. The modiolar sections were obtained in every third section and five sections were randomly selected from each ear (10 sections from each animal). As a result, the LI was measured using 30 sections in each group by a technician naïve to the treatment, preparation techniques or the aims of the current study. To investigate differences among the cochlear turns, the LIs in the basal, second and third turns were also measured 1 and 6 h after application. The LIs of the SGCs, SV and SL 6 h after the application of TAT-myc-FNK onto the RWM, as well as those in the controls, were also measured. To compare the immunostaining intensity among the cells in these organs, the ratios of normalized immunoreactivity were calculated by dividing the LIs at 6 h by those of the control.

### Tympanic injection of TAT-FNK *in vivo*

Eight male albino guinea pigs, weighing 250–300 g and showing ABR thresholds within normal limits based on our laboratory database, were used in this investigation. Only male animals were used because there are gender differences in the ability to detoxify reactive oxygen species and in the levels of endogenous antioxidants in the cochlea.<sup>49,50</sup>

Animals were anesthetized with xylazine hydrochloride (10 mg kg<sup>-1</sup>) and ketamine hydrochloride (40 mg kg<sup>-1</sup>). Chloramphenicol sodium succinate (30 mg kg<sup>-1</sup>, intramuscular injection) was administered as a prophylactic. Under aseptic conditions, the bulla was exposed bilaterally from an occipitolateral approach and opened to allow visualization of the RWM. A gelatin sponge soaked with 3  $\mu$ l of TAT-FNK (6 mg ml<sup>-1</sup>) was placed on the RWM in the left ear, whereas a gelatin sponge soaked with only a vehicle was placed on the RWM in the right ear. One hour after the wound was sutured, a single dose of KM (200 mg kg<sup>-1</sup>; Meiji, Tokyo, Japan)

was injected subcutaneously. Then, 2 h after the KM injection, the jugular vein was exposed under general anesthesia and EA ( $40 \text{ mg kg}^{-1}$ ; Sigma-Aldrich, Tokyo, Japan) was infused into the vein as described previously.<sup>51</sup> An additional four animals served as drug controls: a gelatin sponge soaked with  $3 \mu\text{l}$  of TAT-FNK ( $6 \text{ mg ml}^{-1}$ ) was placed on the left RWM, but KM and EA were not administered.

#### ABR measurement

ABRs were recorded using waveform storing and stimulus control using MEB-5504 (NIHON KOHODEN CO., Tokyo Japan) and DPS-725 (DIA MEDICAL CO., Tokyo, Japan). Sound stimuli were produced by the PT-R7 III ribbon-type speaker (PIONEER CO., Tokyo, Japan). Recordings were performed in a closed-field TRACOUSTICS acoustic enclosure (TRACOUSTICS INC., Austin, TX, USA) and sound level calibration was performed using a sound-level meter (NA-28 RION, Tokyo, Japan). Pure tones (4, 8 and 20 kHz) were measured 3 days after the arrival of the animals to determine the baseline thresholds, and 14 days after the ototoxic insult (for experimental animals) or TAT-FNK application (for drug control animals) to determine the threshold shifts. The frequencies (4, 8 and 20 kHz) measured in this study were frequently used for other studies using guinea pigs, including our previous study.<sup>13,52,53</sup> We have limited our investigation to these frequencies to evaluate hearing to minimize the stress on these animals. The method of ABR measurement has been described previously.<sup>54</sup> In brief, animals were anesthetized with a mixture of xylazine hydrochloride ( $10 \text{ mg kg}^{-1}$ , intramuscular) and ketamine hydrochloride ( $40 \text{ mg kg}^{-1}$ , intramuscular), and needle electrodes were placed subcutaneously at the vertex (active electrode), beneath the pinna of the measured ear (reference electrode) and beneath the opposite ear (ground). The stimulus duration was 15 ms, with a presentation rate of  $11 \text{ s}^{-1}$ , and the rise/fall time was 1 ms. Responses of 1024 sweeps were averaged at each intensity level (5-dB steps) to assess the threshold. The threshold was defined as the lowest intensity level at which a clear reproducible waveform was visible in the trace. When an ABR waveform could not be evoked, the threshold was assumed to be 5 dB greater than the maximum intensity produced by the system (105 dB SPL). Threshold shifts were calculated by subtracting the baseline thresholds from those observed before killing.

#### Assessment of extent of HC loss

After ABR measurements 14 days after ototoxic insults (experimental animals) or TAT-FNK application (drug control animals), animals were killed under deep anesthesia using xylazine hydrochloride and ketamine hydrochloride. The bilateral cochleae were perfused with 4% paraformaldehyde in 0.1 M PBS at pH 7.4 through the oval and round windows, and then immersed in the same fixative overnight at  $4^\circ\text{C}$ . The cochleae were then washed with PBS, permeabilized with 0.3% Triton X-100 for 10 min and labeled with 1% rhodamine phalloidin (Molecular Probes, Eugene, OR, USA) for 30 min to stain F-actin. The tissues were processed as whole mounts using the surface preparation technique. The specimens were then mounted on glass slides using the Prolong Antifade kit (Molecular Probes) and observed. Reticules whose length (bin width) at  $\times 40$  was 0.45 mm were used to count the numbers of total and missing HCs. HCs that showed an identifiable cell body and cuticular plate were considered to be present. The presence of distinctive scar formations produced by convergence of adjacent phalangeal processes was regarded as an indicator of a missing HC. The percentage of HC loss for the IHCs and OHCs was calculated for each segment obtained from each animal. The average for each segment was then determined for each group and plotted from the apex to the base to produce an average cytochleogram. Two animals were excluded because of tissue damage during surface preparation, leaving a total of six cochleae for the HC count study.

#### Assessment of the protective effects of TAT-FNK and caspase-9 detection for cultured HCs

Sprague-Dawley rats (Saitama Experimental Animals Supply Co. Ltd) were decapitated on postnatal day 5 (P5) and the cochlea was carefully dissected out. On the basis of the methods of Sobkowicz *et al.*,<sup>55</sup> the SV,

the SL and the spiral ganglion neurons were dissected away, leaving the OC. The cochlea used for analysis was prepared by cutting 2 mm from the basal end and 3 mm from the apical end of the cochlea (approximately half of the cochlea). Explants were maintained in Dulbecco's modified Eagle's medium with 10% fetal bovine serum, 25 mM HEPES and  $30 \text{ U ml}^{-1}$  penicillin, and were cultured in an incubator at  $37^\circ\text{C}$  under 5%  $\text{CO}_2$  and 95% humidity for 24 h. Explants were exposed to medium containing 20 nM TAT-FNK, 20 nM FNK without TAT or vehicle. Two hours after exposure, the medium was changed to one containing 6 mM KM and either 20 nM FNK, 20 nM TAT-FNK or the vehicle. Typically, 10 cultures were evaluated for each experimental condition: four were cultured for 10 h for detection of caspase-9 and six were cultured for 12 h for cell counting. Additional 10 cultures were evaluated for control, of which four were cultured for 10 h and six were cultured for 12 h, with the medium containing no KM.

Caspase-9 activity was examined by using the fluorescent caspase substrate fam-LEHD-fmk (caspase-9 substrate), which was obtained from Intergen (Purchase, NY, USA) and used according to the manufacturer's protocol. After culturing, the fluorescent substrate was added directly to the culture medium (final concentration,  $5 \mu\text{M}$ ) for the final hour in culture. After 1 h in this substrate, the OC was washed three times for 15 min each at  $37^\circ\text{C}$  in the washing buffer supplied by the manufacturer. The cultures were then fixed overnight at  $4^\circ\text{C}$  in the fixative supplied by the manufacturer. After fixation, the cochleae were washed with PBS, permeabilized with 0.3% Triton X-100 for 10 min and labeled with 1% rhodamine phalloidin (Molecular Probes) for 30 min to stain F-actin. Whole mounted cochleae were viewed with a confocal laser-scanning microscope (ZEISS LSM5 PASCAL). Caspase-9-positive cells were counted over a 0.2 mm longitudinal distance from four separate regions in each culture. A mean value was determined for each culture.

For HC counting, cultures were fixed overnight at  $4^\circ\text{C}$  in the fixative supplied by the manufacturer. After fixation, the cochleae were washed with PBS, permeabilized with 0.3% Triton X-100 for 10 min and labeled with 1% rhodamine phalloidin (Molecular Probes) for 30 min to stain F-actin. To quantify HC loss in the cochlea after various treatments, IHCs and OHCs were counted over a 0.2 mm longitudinal distance from four separate regions of each culture. A mean value was determined for each culture.

#### Statistical analysis

The SPSS software was used for statistical analysis. The time course of the LI for TAT-myc-FNK in the OC was compared between groups by one-way and then pairwise comparisons, with statistical significance adjusted for multiple comparisons (Scheffe's test). The differences in the turns of the LI for TAT-myc-FNK in the OC at 1 and 6 h were compared by two-way ANOVA (the independent variables were cochlear turns and time course). The differences in the normalized LIs between the sub-sites in the cochlea were compared by one-way ANOVA, and then pairwise comparisons were performed by using Scheffe's test. The ABR thresholds at each frequency before and 14 days after the ototoxic insults were compared by two-way ANOVA (the independent variables were TAT-FNK administration and hearing frequency). The extent of missing HCs *in vitro* was also compared by two-way ANOVA (the independent variables were TAT-FNK treatment and type of HC). Caspase-9 activities between the groups were compared by one-way ANOVA followed by Scheffe's test. The extent of missing HCs *in vitro* after exposure to KM was compared by two-way ANOVA (the independent variables were type of HC and drug administration), and if a statistically significant interaction was observed, Bonferroni test was used for simple effects analysis. A level of  $P < 0.05$  was accepted as statistically significant.

#### CONFLICT OF INTEREST

The authors declare no conflict of interest.

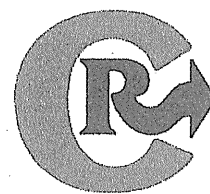
#### ACKNOWLEDGEMENTS

We thank Ms A Tsuyuzaki and Ms Y Kurasawa (Department of Otolaryngology and Head and Neck Surgery, Faculty of Medicine, University of Tokyo, Tokyo, Japan) for technical assistance. This work was supported by Grants (17659527 and 20390440)

from the Ministry of Education, Culture, Sports, Science, and Technology of Japan to TY and a Grant (15110201) from the Ministry of Health, Labor and Welfare of Japan to TY.

## REFERENCES

- Cheng AG, Cunningham LL, Rubel EW. Mechanisms of hair cell death and protection. *Curr Opin Otolaryngol Head Neck Surg* 2005; **13**: 343–348.
- Rybak LP, Whitworth CA, Mukherjee D, Ramkumar V. Mechanisms of cisplatin-induced ototoxicity and prevention. *Hear Res* 2007; **226**: 157–167.
- Rizzi MD, Hirose K. Aminoglycoside ototoxicity. *Curr Opin Otolaryngol Head Neck Surg* 2007; **15**: 352–357.
- Staecker H, Liu W, Malgrange B, Lefebvre PP, Van De Water TR. Vector-mediated delivery of bcl-2 prevents degeneration of auditory hair cells and neurons after injury. *ORL J Otorhinolaryngol Relat Spec* 2007; **69**: 43–50.
- Liu YH, Ke XM, Qin Y, Gu ZP, Xiao SF. Adeno-associated virus-mediated Bcl-xL prevents aminoglycoside-induced hearing loss in mice. *Chin Med J* 2007; **120**: 1236–1240.
- Haas R, Murea S. The role of granulocyte colony-stimulating factor in mobilization and transplantation of peripheral blood progenitor and stem cells. *Cytokines Mol Ther* 1995; **1**: 249–270.
- Schwarze SR, Ho A, Vocero-Akbani A, Dowdy SF. *In vivo* protein transduction: delivery of a biologically active protein into the mouse. *Science* 1999; **285**: 1569–1572.
- Becker-Hapak M, McAllister SS, Dowdy SF. TAT-mediated protein transduction into mammalian cells. *Methods* 2001; **24**: 247–256.
- Asoh S, Ohtsu T, Ohta S. The super antiapoptotic factor Bcl-xFNK constructed by disturbing intramolecular polar interactions in rat Bcl-xL. *J Biol Chem* 2000; **275**: 37240–37245.
- Asoh S, Mori T, Nagai S, Yamagata K, Nishimaki K, Miyato Y et al. Zonal necrosis prevented by transduction of the artificial anti-death FNK protein. *Cell Death Differ* 2005; **12**: 384–394.
- Asoh S, Ohsawa I, Mori T, Katsura K, Hiraide T, Katayama Y et al. Protection against ischemic brain injury by protein therapeutics. *Proc Natl Acad Sci USA* 2002; **99**: 17107–17112.
- Nagai S, Asoh S, Kobayashi Y, Shidara Y, Mori T, Suzuki M et al. Protection of hepatic cells from apoptosis induced by ischemia/reperfusion injury by protein therapeutics. *Hepato Res* 2007; **37**: 133–142.
- Kashio A, Sakamoto T, Suzukawa K, Asoh S, Ohta S, Yamasoba T. A protein derived from the fusion of TAT peptide and FNK, a Bcl-x(L) derivative, prevents cochlear hair cell death from aminoglycoside ototoxicity *in vivo*. *J Neurosci Res* 2007; **85**: 1403–1412.
- Minn AJ, Boise LH, Thompson CB. Expression of Bcl-xL and loss of p53 can cooperate to overcome a cell cycle checkpoint induced by mitotic spindle damage. *Genes Dev* 1996; **10**: 2621–2631.
- Valera ET, Brassesco MS, Scrideli CA, Tone LG. Tetraploidization in Wilms tumor in an infant. *Genet Mol Res* 2010; **9**: 1577–1581.
- Schuknecht HF. Ablation therapy for the relief of Meniere's disease. *Trans Am Laryngol Rhinol Otol Soc* 1956; **66**: 589–600.
- Haynes DS, O'Malley M, Cohen S, Watford K, Labadie RF. Intratympanic dexamethasone for sudden sensorineural hearing loss after failure of systemic therapy. *Laryngoscope* 2007; **117**: 3–15.
- Tsuji J, Liberman MC. Intracellular labeling of auditory nerve fibers in guinea pig: central and peripheral projections. *J Comp Neurol* 1997; **381**: 188–202.
- Tanaka K, Motomura S. Permeability of the labyrinthine windows in guinea pigs. *Arch Otorhinolaryngol* 1981; **233**: 67–73.
- Bellucci RJ, Fisher EG, Rhodin J. Ultrastructure of the round window membrane. *Laryngoscope* 1972; **82**: 1021–1026.
- Carpenter AM, Muchow D, Goycoolea MV. Ultrastructural studies of the human round window membrane. *Arch Otolaryngol Head Neck Surg* 1989; **115**: 585–590.
- Miriszlai E, Benedeczyk I, Horváth K, Köllner P. Ultrastructural organization of the round window membrane in the infant human middle ear. *ORL J Otorhinolaryngol Relat Spec* 1983; **45**: 29–38.
- Goycoolea MV, Lundman L. Round window membrane. Structure function and permeability: a review. *Microsc Res Tech* 1997; **36**: 201–211.
- Lundman LA, Holmquist B, Bagger-Sjoberg D. Round window membrane permeability. An *in vitro* model. *Acta Otolaryngol* 1987; **104**: 472–480.
- Juhn SK, Hamaguchi Y, Goycoolea M. Review of round window membrane permeability. *Acta Otolaryngol Suppl* 1989; **457**: 43–48.
- Smith BM, Myers MG. The penetration of gentamicin and neomycin into perilymph across the round window membrane. *Otolaryngol Head Neck Surg* 1979; **87**: 888–891.
- Brady DR, Pearce JP, Juhn SK. Permeability of round window membrane to 22Na or RISA. *Arch Otorhinolaryngol* 1976; **214**: 183–184.
- Nomura Y. Otolological significance of the round window. *Adv Otorhinolaryngol* 1984; **33**: 1–162.
- Morizono T, Hamaguchi Y, Juhn SK. Permeability of human serum albumin from chinchilla middle ear to inner ear. In *XXIII workshop on inner ear biology 1986*. GDR: Berlin.
- Goycoolea MV, Paparella MM, Goldberg B, Carpenter AM. Permeability of the round window membrane in otitis media. *Arch Otolaryngol* 1980; **106**: 430–433.
- Richard JP, Melikov K, Vives E, Ramos C, Verbeure B, Gait MJ et al. Cell-penetrating peptides. A reevaluation of the mechanism of cellular uptake. *J Biol Chem* 2003; **278**: 585–590.
- Vivès E, Brodin P, Lebleu B. A truncated HIV-1 Tat protein basic domain rapidly translocates through the plasma membrane and accumulates in the cell nucleus. *J Biol Chem* 1997; **272**: 16010–16017.
- Wadia JS, Dowdy SF. Protein transduction technology. *Curr Opin Biotechnol* 2002; **13**: 52–56.
- Gupta B, Levchenko TS, Torchilin VP. Intracellular delivery of large molecules and small particles by cell-penetrating proteins and peptides. *Adv Drug Deliv Rev* 2005; **57**: 637–651.
- Ruel-Gariepy E, Chenite A, Chaput C, Guirguis S, Leroux J. Characterization of thermosensitive chitosan gels for the sustained delivery of drugs. *Int J Pharm* 2000; **203**: 89–98.
- Park AH, Jackson A, Hunter L, McGill L, Simonsen SE, Alder SC et al. Cross-linked hydrogels for middle ear packing. *Otol Neurotol* 2006; **27**: 1170–1175.
- Husmann KR, Morgan AS, Girod DA, Durham D. Round window administration of gentamicin: a new method for the study of ototoxicity of cochlear hair cells. *Hear Res* 1998; **125**: 109–119.
- Okamoto T, Yamamoto Y, Gotoh M, Huang CL, Nakamura T, Shimizu Y et al. Slow release of bone morphogenetic protein 2 from a gelatin sponge to promote regeneration of tracheal cartilage in a canine model. *J Thorac Cardiovasc Surg* 2004; **127**: 329–334.
- Salt AN. Simulation of methods for drug delivery to the cochlear fluids. *Adv Otorhinolaryngol* 2002; **59**: 140–148.
- Imamura S, Adams JC. Distribution of gentamicin in the guinea pig inner ear after local or systemic application. *J Assoc Res Otolaryngol* 2003; **4**: 176–195.
- Zou J, Saulnier P, Perrier T, Zhang Y, Manninen T, Toppila E et al. Distribution of lipid nanocapsules in different cochlear cell populations after round window membrane permeation. *J Biomed Mater Res B Appl Biomater* 2008; **87**: 10–18.
- Khalil IA, Kogure K, Akita H, Harashima H. Uptake pathways and subsequent intracellular trafficking in nonviral gene delivery. *Pharmacol Rev* 2006; **58**: 32–45.
- Chen Y, Huang WG, Zha DJ, Qiu JH, Wang JL, Sha SH, Schacht J. Aspirin attenuates gentamicin ototoxicity: from the laboratory to the clinic. *Hear Res* 2007; **226**: 178–182.
- Pruska EM, Schacht J. Mechanism and prevention of aminoglycoside ototoxicity: outer hair cells as targets and tools. *J Ear Nose Throat J* 1997; **76**: 164–166, 168, 170–1.
- Cunningham LL, Cheng AG, Rubel EW. Caspase activation in hair cells of the mouse utricle exposed to neomycin. *J Neurosci* 2002; **22**: 8532–8540.
- Hirose K, Westrum LE, Stone JS, Zirpel L, Rubel EW. Dynamic studies of ototoxicity in mature avian auditory epithelium. *Ann NY Acad Sci* 1999; **884**: 389–409.
- Li Y, Huang Y, Luo S. Alteration of intracellular Ca<sup>2+</sup> caused by streptomycin in the isolated cochlear OHC. *Zhonghua Er Bi Yan Hou Ke Za Zhi* 1995; **30**: 227–229.
- Lehr HA, Mankoff DA, Corwin D, Santeusano G, Gown AM. Application of Photoshop-based image analysis to quantification of hormone receptor expression in breast cancer. *J Histochem Cytochem* 1997; **45**: 1559–1565.
- Julicher RH, Sterrenberg L, Haenen GR, Bast A, Noordhoek J. Sex differences in the cellular defence system against free radicals from oxygen or drug metabolites in rat. *Arch Toxicol* 1984; **56**: 83–86.
- el Barbary A, Altschuler RA, Schacht J. Glutathione S-transferases in the organ of Corti of the rat: enzymatic activity, subunit composition and immunohistochemical localization. *Hear Res* 1993; **71**: 80–90.
- Yamasoba T, Kondo K. Supporting cell proliferation after hair cell injury in mature guinea pig cochlea *in vivo*. *Cell Tissue Res* 2006; **325**: 23–31.
- Suzuki M, Yagi M, Brown JN, Miller AL, Miller JM, Raphael Y. Effect of transgenic GDNF expression on gentamicin-induced cochlear and vestibular toxicity. *Gene Ther* 2000; **7**: 1046–1054.
- Lin CD, Oshima T, Oda K, Yamauchi D, Tsai MH, Kobayashi T. Ototoxic interaction of kanamycin and 3-nitropropionic acid. *Acta Otolaryngol* 2008; **128**: 1280–1285.
- Pourbakhht A, Yamasoba T. Ebselen attenuates cochlear damage caused by acoustic trauma. *Hear Res* 2003; **181**: 100–108.
- Sobkowicz HM, Loftus JM, Slapnick SM. Tissue culture of the organ of Corti. *Acta Otolaryngol Suppl* 1993; **502**: 3–36.



## Micellization of cisplatin (NC-6004) reduces its ototoxicity in guinea pigs

Miyuki Baba <sup>a,b</sup>, Yu Matsumoto <sup>a,b</sup>, Akinori Kashio <sup>a</sup>, Horacio Cabral <sup>c</sup>, Nobuhiro Nishiyama <sup>b</sup>, Kazunori Kataoka <sup>b,c,d,e</sup>, Tatsuya Yamasoba <sup>a,\*</sup>

<sup>a</sup> Department of Otolaryngology and Head and Neck Surgery, Faculty of Medicine, Graduate School of Medicine, Hongo 7-3-1, Bunkyo-Ku, Tokyo, 113-8655, Japan

<sup>b</sup> Division of Clinical Biotechnology, Center for Disease Biology and Integrative Medicine, Graduate School of Medicine, Hongo 7-3-1, Bunkyo-Ku, Tokyo, 113-8655, Japan

<sup>c</sup> Department of Bioengineering, Graduate School of Engineering, Hongo 7-3-1, Bunkyo-Ku, Tokyo, 113-8655, Japan

<sup>d</sup> Department of Materials Engineering, Graduate School of Engineering, Hongo 7-3-1, Bunkyo-Ku, Tokyo, 113-8655, Japan

<sup>e</sup> Center for NanoBio Integration, University of Tokyo, Hongo 7-3-1, Bunkyo-Ku, Tokyo, 113-8655, Japan

### ARTICLE INFO

#### Article history:

Received 3 February 2011

Accepted 17 July 2011

Available online 23 July 2011

#### Keywords:

Auditory brainstem response

Cisplatin

Guinea pig

Hair cell

Polymeric micelle

Ototoxicity

### ABSTRACT

Nanocarriers potentially reduce or prevent chemotherapy-induced side effects, facilitating the translation of nanocarrier formulation into the clinic. To date, organ-specific toxicity by nanocarriers remains to be clarified. Here, we studied the potential of polymeric micelle nanocarriers to prevent the ototoxicity, which is a common side effect of high-dose cisplatin (CDDP) therapy. In this study, we evaluated the ototoxicity of CDDP-incorporating polymeric micelles (NC-6004) in guinea pigs in comparison with that of cisplatin. Their auditory brainstem responses (ABRs) to 2, 6, 12, 20, and 30 kHz sound stimulation were measured before and 5 days after the drug administration. Groups treated with NC-6004 showed no apparent ABR threshold shifts, whereas groups treated with CDDP showed dose-dependent threshold shifts particularly at the higher frequencies. Consistent with the ABR results, groups treated with NC-6004 showed excellent hair-cell preservation, whereas groups treated with CDDP exhibited significant hair-cell loss ( $P < 0.05$ ). Synchrotron radiation-induced X-ray fluorescence spectrometry imaging demonstrated that the platinum distribution and concentration in the organ of Corti were significantly reduced ( $P < 0.01$ ) in guinea pigs treated with NC-6004 compared with guinea pigs treated with CDDP. These findings indicate that micellization of CDDP reduces its ototoxicity by circumventing the vulnerable cells in the inner ear.

© 2011 Elsevier B.V. All rights reserved.

### 1. Introduction

Recently, nanocarrier-mediated drug delivery has received great attention in cancer therapy since nanocarriers carrying chemotherapeutic agents have shown to enhance antitumor activity with reduced side effects [1–4]. The antitumor activity is enhanced because the tumor accumulation is augmented in the nanocarriers via the enhanced permeability and retention (EPR) effect [5], which is based on the following pathophysiological characteristics of solid tumors: hypervascularity, incomplete vascular architecture, secretion of vascular permeability factors stimulating extravasation within the cancer tissue, and the absence of effective lymphatic drainage. However, the reduction or prevention of chemotherapy-induced side effects, especially organ-specific toxicity, by nanocarriers remains to be completely clarified. The mechanisms of nanocarrier-mediated reduction of chemotherapy-induced organ-specific toxicity must be

shown to facilitate the translation of nanocarrier formulation into the clinic.

Polymeric micelles, which are self-assemblies of block copolymers, have gained increasing popularity as nanocarriers for chemotherapeutic agents since their critical features, including size and drug loading and release, can be modulated by engineering block copolymers. Polymeric micelles carrying chemotherapeutic agents can selectively and effectively accumulate in the solid tumors, thereby leading to enhanced antitumor activity. Currently, our micelle formulations of paclitaxel (PTX), SN-38 (a biologically active metabolite of CPT-11), cisplatin (*cis*-dichlorodiammineplatinum(II), CDDP), and 1,2-diaminocyclohexane (DACHPt) are being tested in clinical trials. Regarding chemotherapy-induced side effects, polymeric micelles have been revealed to restrain the neurotoxicity of PTX and CDDP [6,7], intestinal toxicity of CPT-11 [8], and the nephrotoxicity of CDDP [7].

CDDP is a common chemotherapeutic agent used to treat many different types of cancer, including lung, gastrointestinal, bladder, and head and neck cancer. The major dose-limiting factors in CDDP therapy is the nephrotoxicity, which can be reversed to some extent by increasing the saline hydration and by using diuretic agents. As aforementioned, micellization of CDDP can prevent the nephrotoxicity,

\* Corresponding author at: Department of Otolaryngology and Head and Neck Surgery, Graduate School of Medicine, University of Tokyo, Hongo 7-3-1, Bunkyo-ku, Tokyo 113-8655, Japan. Tel.: +81 3 5800 8924; fax: +81 3 3814 9486.

E-mail address: tyamasoba-ky@umin.ac.jp (T. Yamasoba).